

Digital Processing of Conical Scanner Data

Skylab S-192 conical scanner data, digitally processed to remove systematic errors, were recorded on film and provided imagery of good quality.

INTRODUCTION

IN THE PAST, the correction of earth observation image data has been done primarily with electro-optical image processing techniques¹. Extensive research in digital processing has been conducted^{2,3,4}. Digital processing of earth observation sensor data is now accepted as the best technology for geometric and radiometric correction⁵.

Most of the work that has been performed has dealt with linear scanners^{2,3,4}. A class of instruments that scan the earth along a curved path (as opposed to a linear path) is that of the conical scanners. They have unique geometric properties that require a different approach to correction⁶. This paper presents the techniques and results of a recent investigation in which Skylab S-192 conical data was geometrically corrected, by using digital image processing methods, in order to eliminate systematic errors.

ABSTRACT: An experimental software system to remove systematic errors and to geometrically correct S-192 conical scanner data by using digital techniques has been developed. The digital image processing programs were implemented on an IBM 370/168 computer and were used on a September 15, 1973 S-192 image of Lake Havasu, Arizona. The resulting digital image was recorded on film and was of good quality. The experiment described demonstrates that digital image processing techniques can be used to correct conical scanner data.

STATEMENT OF PROBLEM

The principal objective of the experiment described in this paper is to show that conical scanner data can be geometrically corrected by using digital techniques. A second objective is to determine ways for minimizing the computer resources required to geometrically correct conical scanner data.

BACKGROUND

The S-192 multispectral scanner is an optical-mechanical scanner, together with a spectral dispersion system. It uses a rotating mirror to perform a conical scanning of the earth. The cone angle is 5° 32' about the instrument axis. Data are collected during the front 116° 15' of the 360° scanning cycle. There are 13 detectors which cover spectral regions with wavelengths be-

tween 0.41 and 12.5 micrometers⁶. The scan geometry of the conical scanner is shown in Figure 1, where

γ is the cone angle,

η is the scan angle,

V is the spacecraft position, and

\overline{VP} is the vector along which the sensor points.

The rectangular coordinate axes represent the local sensor coordinate system (see Appendix A for definitions of all coordinate systems used in this paper). As the point P moves around a circle which is perpendicular to the Z_s -axis, the line VP generates a cone (hence, the term "conical scanner").

The input data used in this experiment consisted of type 51-2 computer-compatible tapes⁷. These processed data tapes contain GMT-correlated calculated aperture radiances, as well as some ancillary data. That is, the data have been radiometrically corrected but not geometrically corrected.

OUTLINE OF EXPERIMENT

The presence of the S-192 conical scanner on Skylab provided a unique opportunity to use real conical data in this experiment. The processing was done in the five steps shown in Figure 2. These same steps were used in demonstrating all-digital processing of LANDSAT-1 MSS data⁴. Each step will be described.

DATA REFORMATTING

There were two reasons for reformatting the input data. First, the type 51-2 computer-compatible tape format is not usable by the geometric correction program. It was much simpler to write a reformatting program than it would have been to modify the geometric correction program. Second, it was necessary to strip the ancillary data from the type 51-2 tape and to save it on a direct access data set for use by the error modeling program. Consequently, a computer program that reformats the data was written. Each record contains data from all spectral bands in line-interleaved format.

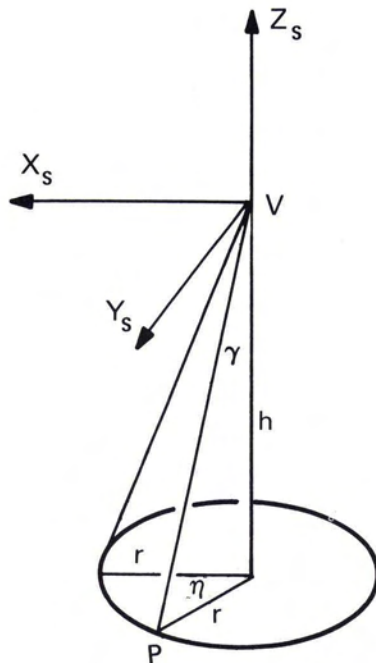


FIG 1. Conical scan geometry.

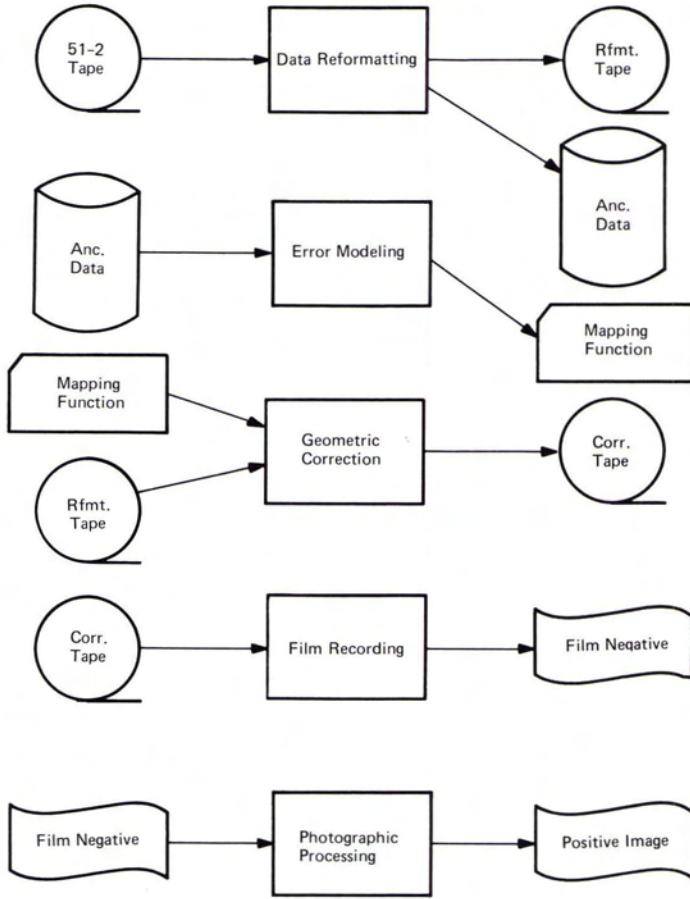


FIG 2. S-192 processing steps and data flow.

ERROR MODELING

The output image is defined to be a rectangular array of square pixels. Each output-image pixel represents a square of 50.8 metres in length and width. The particular pixel size was chosen so that the resulting film products will be at a scale of 1:500,000 when recorded on an IBM Drun Scanner/Plotter. The output image represents a Universal Transverse Mercator (UTM) projection. The input image is a rectangular array of pixels taken from a type 51-2 tape.

The function of the error modeling program is to create an output-image to input-image mapping function as indicated in Figure 3. The domain of the mapping function consists of

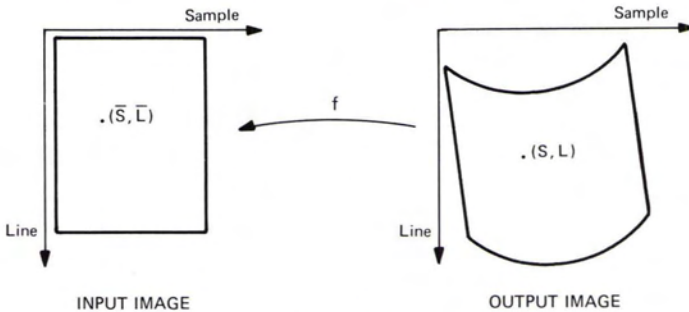


FIG 3. Output-image to input-image mapping function.

locations (i.e., line and sample coordinates) in the output image, and the range of the mapping function consists of locations in the input image. An output-image is physically created by using the mapping function to aid in computing the intensity (radiance) of each output-image pixel. The function is evaluated at an output-image pixel location (S, L). The intensities of the pixels near the resulting input-image location (\bar{S}, \bar{L}) are used in an appropriate resampling algorithm to compute the intensity of the out-put image pixel (S, L). The computer program which performed the error modeling for the experiment was written in FORTRAN and was compiled with a FORTRAN IV H EXTENDED compiler. Essentially all computations are done with 8-byte floating-point arithmetic. The main transformations which make up the error modeling program are all done in the subroutines described below.

INITIALIZATION

The initialization routines, in addition to reading various input parameters, define an array of points in the input-image space. These points, called anchor points, are regularly spaced 100 pixels apart as illustrated in Figure 4. In the actual image that was processed, there were 15 columns and 20 rows of anchor points (a total of 300 anchor points). Pixel coordinates (sample number and line number) are used for the input-image anchor points.

INPUT IMAGE TO SCAN ANGLE AND ANCILLARY PARAMETERS

The input-image sample coordinate of each anchor point is used to calculate the scan angle of that point:

$$\eta = \left(\bar{S} - \frac{N' + 1}{2} \right) \left(\frac{W\pi}{180(N' - 1)} \right) \quad (1)$$

where

η is the scan angle measured counter clockwise from the satellite velocity vector (as shown in Figure 1) in radians,

\bar{S} is the sample coordinate in pixels,

N' equals 1240 which is equal to the number of samples in one input scan line, and

W equals 116.25 which is equal to the total scanning arc width in degrees.

All calculations in Equation 1 are done in 8-byte floating-point arithmetic.

The input-image line coordinate of each anchor point is used to obtain certain ancillary parameters that were originally on the type 51-2 input data tape. The following parameters are used by the error modeling programs:

- Satellite roll
- Satellite pitch
- Satellite yaw
- Nadir latitude
- Nadir longitude
- Spacecraft altitude
- Orbital inclination angle

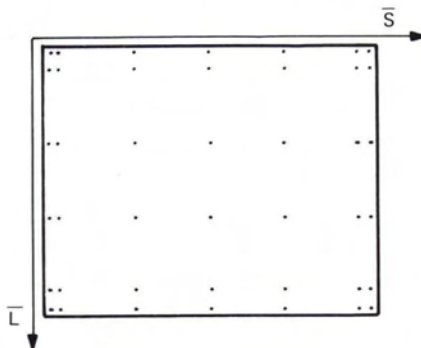


FIG. 4. Input-image anchor points.

These seven values correspond to the time at which the first sample of the given line was observed. There is a set of ancillary parameters for each scan line.

SCAN ANGLE AND ANCILLARY PARAMETERS TO GEODETIC LATITUDE AND LONGITUDE

This routine computes the geodetic latitude and longitude of each anchor point. The treatment used essentially is that of Eppes⁸. In Figure 1, the S-192 instrument is assumed to be pointing along the line VP . The coordinates of the intersection of the line VP with the earth ellipsoid are computed. From these coordinates, the geodetic latitude and longitude are calculated.

In order to compute the intersection of the line VP and the earth ellipsoid, it is necessary to have the equations of both the line and the ellipsoid with respect to the same coordinate system. These are obtained by first finding the equation of the line in local sensor coordinates and then using several coordinate transformations to get the equation of the line in local earth-centered coordinates. (See Appendix A for definitions of coordinate systems.)

The equation of the line VP has the form

$$\frac{X_s}{A'} = \frac{Y_s}{B'} = \frac{Z_s}{C'} \quad (2)$$

in local sensor coordinates. The coordinates of the point P are $(r \cos \eta, r \sin \eta, -h)$. Hence, the direction cosines in Equation 2 are

$$\begin{aligned} A' &= \frac{(1,0,0) \cdot \overline{VP}}{|\overline{VP}|} = \frac{r \cos \eta}{h^2 + r^2} = \sin \gamma \cos \eta \\ B' &= \frac{(0,1,0) \cdot \overline{VP}}{|\overline{VP}|} = \frac{r \sin \eta}{h^2 + r^2} = \sin \gamma \sin \eta \\ C' &= \frac{(0,0,1) \cdot \overline{VP}}{|\overline{VP}|} = \frac{-h}{h^2 + r^2} = -\cos \gamma \end{aligned}$$

The equation of the line VP can also be written in the parametric form:

$$\begin{aligned} X_s &= p \sin \gamma \cos \eta = pA' \\ Y_s &= p \sin \gamma \sin \eta = pB' \\ Z_s &= -p \cos \gamma = pC' \end{aligned} \quad (3)$$

The equation of the line VP in local earth-perpendicular coordinates will now be found. The attitude transformation matrix can be written in the form

$$\begin{aligned} A &= \begin{bmatrix} \cos AP & 0 & -\sin AP \\ 0 & 1 & 0 \\ \sin AP & 0 & \cos AP \end{bmatrix} \begin{bmatrix} 1 & 0 & 0 \\ 0 & \cos AR & \sin AR \\ 0 & -\sin AR & \cos AR \end{bmatrix} \begin{bmatrix} \cos AY & \sin AY & 0 \\ -\sin AY & \cos AY & 0 \\ 0 & 0 & 1 \end{bmatrix} \\ &= (a_{ij}). \end{aligned}$$

where

AP is the pitch angle (right-handed rotation about the Yp -axis),
 AR is the roll angle (right-handed rotation about the Xp -axis), and
 AY is the yaw angle (right-handed rotation about the Zp -axis).

Then the coordinate transformation equation is

$$\begin{bmatrix} X_s \\ Y_s \\ Z_s \end{bmatrix} = A \begin{bmatrix} X_p \\ Y_p \\ Z_p \end{bmatrix} \quad (4)$$

The Cramer matrices $A1$, $A2$, $A3$, are defined:

$$A1 = \begin{bmatrix} A' & a_{12} & a_{13} \\ B' & a_{22} & a_{23} \\ C' & a_{32} & a_{33} \end{bmatrix}$$

$$A2 = \begin{bmatrix} a_{11} & A' & a_{13} \\ a_{21} & B' & a_{23} \\ a_{31} & C' & a_{33} \end{bmatrix}$$

$$A3 = \begin{bmatrix} a_{11} & a_{12} & A' \\ a_{21} & a_{22} & B' \\ a_{31} & a_{32} & C' \end{bmatrix}$$

Then Equation 4 has the solution:

$$\begin{aligned} Xp &= p(|A1|/|A|) = p|A1| \\ Yp &= p(|A2|/|A|) = p|A2| \\ Zp &= p(|A3|/|A|) = p|A3| \end{aligned} \quad (5)$$

since $|A| = 1$. After algebraic manipulation, Equation 5 can be written in the form

$$C_1 Xp = C_2 Yp = C_3 Zp \quad (6)$$

where

$$\begin{aligned} C_1 &= |A2| |A3| \\ C_2 &= |A1| |A3| \\ C_3 &= |A1| |A2| \end{aligned}$$

The equation of the line VP in local earth-tangent coordinates is derived from the transformation:

$$\begin{bmatrix} Xp \\ Yp \\ Zp \end{bmatrix} = \begin{bmatrix} Xt \\ Yt \\ Zt - H \end{bmatrix} \quad (7)$$

where H is the spacecraft altitude measured along a perpendicular to the earth ellipsoid. Substituting Equation 7 into Equation 6 gives the resulting equation of the line VP in local earth-tangent coordinates:

$$C_1 Xt = C_2 Yt = C_3 (Zt - H). \quad (8)$$

The final transformation of the equation of the line VP will be to local earth-centered coordinates. The transformation consists of a translation followed by two rotations. The azimuth rotation matrix

$$AZM = \begin{bmatrix} \cos AZS & -\sin AZS & 0 \\ \sin AZS & \cos AZS & 0 \\ 0 & 0 & 1 \end{bmatrix}$$

represents a counter-clockwise rotation through the angle AZS around the Z_c -axis. The geodetic-latitude rotation matrix

$$LDM = \begin{bmatrix} \sin LDN & 0 & -\cos LDN \\ 0 & 1 & 0 \\ \cos LDN & 0 & \sin LDN \end{bmatrix}$$

represents a clockwise rotation through the angle $(\pi/2 - LDN)$ around the Y_c -axis. Then the transformation from local earth-centered coordinates to local earth-tangent coordinates is given by

$$\begin{bmatrix} X_t \\ Y_t \\ Z_t \end{bmatrix} = (AZM) (LDM) \left\{ \begin{bmatrix} X_c \\ Y_c \\ Z_c \end{bmatrix} - \begin{bmatrix} X_{cn} \\ 0 \\ Z_{cn} \end{bmatrix} \right\} \quad (9)$$

where

$$\begin{aligned} AZS &= \arcsin\left(\frac{\cos OIE}{\cos LCN}\right) = \text{instantaneous heading or azimuth measured clockwise from south} \\ OIE &= \text{inclination angle of orbital plane from equator} \\ LCN &= \text{geocentric latitude of the spacecraft nadir} \\ LDN &= \text{geodetic latitude of the spacecraft nadir} \\ X_{cn} &= E \cos LDN \\ Z_{cn} &= E(1-e^2) \sin LDN \end{aligned} \left. \vphantom{\begin{aligned} AZS \\ OIE \\ LCN \\ LDN \\ X_{cn} \\ Z_{cn} \end{aligned}} \right\} \text{ earth-centered coordinates of spacecraft nadir}$$

$$E = \frac{a}{\sqrt{1 - e^2 \sin^2 LDN}}$$

$$e = \frac{\sqrt{a^2 - b^2}}{a} = \text{eccentricity of the earth ellipsoid}$$

$$a = \text{semi-major (equatorial) axis of the earth ellipsoid}$$

$$b = \text{semi-minor (polar) axis of the earth ellipsoid.}$$

If the matrix product $(AZM)(LDM) = (b_{ij})$, then substituting Equation 9 into Equation 8 gives

$$\begin{aligned} &C_1[b_{11}(X_c - X_{cn}) + b_{12}Y_c + b_{13}(Z_c - Z_{cn})] \\ &= C_2[b_{21}(X_c - X_{cn}) + b_{22}Y_c + b_{23}(Z_c - Z_{cn})] \\ &= C_3[b_{31}(X_c - X_{cn}) + b_{32}Y_c + b_{33}(Z_c - Z_{cn}) - H]. \end{aligned} \quad (10)$$

Equations 10 can be written in parametric form with Z_c as the parameter:

$$\begin{aligned} R_1X_c + R_2Y_c &= -R_3Z_c + R_1X_{cn} + R_3Z_{cn} \\ S_1X_c + S_2Y_c &= -S_3Z_c + S_1X_{cn} + S_3Z_{cn} - C_3H \end{aligned} \quad (11)$$

where

$$\begin{aligned} R_1 &= C_1b_{11} - C_2b_{21} \\ R_2 &= C_1b_{12} - C_2b_{22} \\ R_3 &= C_1b_{13} - C_2b_{23} \\ S_1 &= C_1b_{31} - C_3b_{31} \\ S_2 &= C_1b_{32} - C_3b_{32} \\ S_3 &= C_1b_{33} - C_3b_{33} \end{aligned}$$

By using Cramer's rule, Equations 11 can be solved for X_c and Y_c in terms of Z_c (Z_c is regarded as a parameter):

$$\begin{aligned} X_c &= \bar{A}Z_c + \bar{B} \\ Y_c &= \bar{C}Z_c + \bar{D} \end{aligned} \quad (12)$$

where

$$\begin{aligned}\bar{A} &= \frac{R_2S_3 - R_3S_2}{R_1S_2 - R_2S_1} \\ \bar{B} &= \frac{(R_1S_2 - R_2S_1)Xcn + (R_3S_2 - R_2S_3)Zcn + C_3R_2H}{R_1S_2 - R_2S_1} \\ \bar{C} &= \frac{R_3S_1 - R_1S_3}{R_1S_2 - R_2S_1} \\ \bar{D} &= \frac{(R_1S_3 - R_3S_1)Zcn - C_3R_1H}{R_1S_2 - R_2S_1}.\end{aligned}$$

Equations 12 can be substituted into the equation for the earth ellipsoid,

$$\frac{Xc^2 + Yc^2}{a^2} + \frac{Zc^2}{b^2} = 1,$$

to get the following, after collecting terms:

$$(a^2 + b^2\bar{A}^2 + b^2\bar{C}^2)Zc^2 + 2b^2(\bar{A}\bar{B} + \bar{C}\bar{D})Zc - b^2(a^2 - \bar{B}^2 - \bar{D}^2) = 0.$$

By using the quadratic formula:

$$\begin{aligned}d &= b^2(\bar{A}\bar{B} + \bar{C}\bar{D})^2 + (a^2 - \bar{B}^2 - \bar{D}^2)[a^2 + b^2(\bar{A}^2 + \bar{C}^2)] \\ Zc &= \frac{-b^2(\bar{A}\bar{B} + \bar{C}\bar{D}) \pm b\sqrt{d}}{a^2 + b^2(\bar{A}^2 + \bar{C}^2)}.\end{aligned}\quad (13)$$

the Xc and Yc coordinates of the ray-ellipsoid intersection are now calculated by substituting Equation 13 into Equation 12. The positive sign is used in Equation 13 for a northern-hemisphere intersection, and the negative sign is used for a southern-hemisphere intersection.

The local earth-centered coordinates of the intersection of the line VP with the earth ellipsoid are converted to geodetic latitude and longitude by the well-known equations:

$$\begin{aligned}Ld &= \arcsin \sqrt{\frac{Xc^2 + Yc^2 - a^2}{(Xc^2 + Yc^2)e^2 - a^2}} \\ Ln &= Lnn + \arctan\left(\frac{Yc}{Xc}\right)\end{aligned}$$

where

- Lnn is the longitude of the spacecraft nadir,
- Ld is the geodetic latitude of an anchor point, and
- Ln is the longitude of an anchor point.

GEODETIC LATITUDE AND LONGITUDE TO UTM

The geodetic latitude and longitude coordinates of the anchor points are converted to UTM coordinates by means of a modified version of a program obtained from the United States Geological Survey.

UTM TO OUTPUT IMAGE

The array of anchor point UTM coordinates is converted to output-image pixel coordinates by the equation:

$$\begin{bmatrix} S \\ L \end{bmatrix} = \begin{bmatrix} -\sin \alpha & \cos \alpha \\ \cos \alpha & \sin \alpha \end{bmatrix} \begin{bmatrix} \frac{E - E_c}{S_s} \\ \frac{N - N_c}{S_l} \end{bmatrix} + \begin{bmatrix} \frac{W_s}{2} \\ \frac{W_l}{2} \end{bmatrix}$$

where

- α = angle measured clockwise from the positive E -axis to the positive L -axis
- E = UTM easting of an anchor point
- N = UTM northing of an anchor point
- E_c = UTM easting of format center of output image
- N_c = UTM northing of format center of output image
- S_s = width of one output-image pixel = 50.8 metres
- S_l = length of one output-image pixel = 50.8 metres
- W_s = number of samples in one output-image line
- W_l = number of lines in the output image
- S = output-image sample coordinate
- L = output-image line coordinate

MAPPING FUNCTION

The routines described compute the output-image coordinates (S, L) of each of 300 input-image anchor points (\bar{S}, \bar{L}). The mapping function will be two least-squares polynomials, P_s and P_l , of degree 5 (21 terms each) that map each point (S, L) onto the corresponding input-image anchor point (\bar{S}, \bar{L}). That is,

$$\bar{S} = P_s(S, L)$$

$$\bar{L} = P_l(S, L)$$

or, in the notation of Figure 3,

$$f(S, L) = (P_s(S, L), P_l(S, L)).$$

GEOMETRIC CORRECTION

Geometric correction was performed by using the nearest-neighbor assignment algorithm. The technique is adequately described elsewhere^{2,3} and only will be summarized here. Nearest-neighbor assignment means that, for each output-image pixel, the intensity (radiance) of the particular input-image pixel whose location is closest to the location in the input image of that output-image pixel is used. That is, for each output-image pixel location (S, L), the corresponding input-image location (\bar{S}, \bar{L}) is found. Note that S and L are integers, but \bar{S} and \bar{L} usually are not integers. The input-image location (\bar{S}', \bar{L}'), which is the closest point to (\bar{S}, \bar{L}) having integral coordinates, is found. Then the intensity of the Point (\bar{S}', \bar{L}') is used as the intensity of the point (S, L).

Theoretically, the mapping function should be used on every point in the output image. Doing this would be quite expensive computationally. Instead of mapping every point, a rectangular array of points was mapped to the input image. This array of grid points contained 35 rows and 31 columns, totalling 1085 points. The spacing between the rows was 100 pixels, and between the columns it was 50 pixels. The remaining 5,098,915 points of the output image were mapped to the input image by using successive linear interpolations on the grid points. This method is considerably cheaper than the mapping of all 5,100,000 points through the two polynomials would be.

PHOTO PROCESSING

The geometrically corrected image was then recorded on photographic film by using an IBM Drum Scanner/Plotter⁹. These negatives were developed, and positive false-color image products were made from the negatives.

RESULTS AND CONCLUSIONS

The experiment described consisted of systematic geometric correction of Skylab S-192 conical data. The error modeling program ran in 4.77 seconds on an IBM 370/168 computer. The running time for each anchor point is about the same as that of IBM's LANDSAT error

modeling programs. However, since the conical scanner has larger distortions than a linear scanner (due to the curvature of the scan lines), it requires more anchor points than a linear scanner. It is estimated that a conical scanner may require up to twice as much Central Processing Unit (CPU) time as a comparable linear scanner in order to perform the error modeling step. This difference between conical and linear scanners is likely to be insignificant relative to the total correction times.

The geometric correction of the S-192 data confirmed that conical scanner data can be geometrically corrected by the same methods that have been used successfully for linear scanner data. Either type of sensor requires the same amount of computer time per pixel. However, it is necessary to have all of the input-image data needed to construct one output-image line in core at one time. For linear scanner data, whose distortions are on the order of only a few input-image lines, this restriction is negligible. A buffer of 10 or 20 input-image data lines is all that is required. The curvature of a conical scan line dictates that an output-image line be constructed from data from hundreds of input-image scan lines. In the case of Skylab S-192 data, the large buffer required was not prohibitive because there were only 1240 samples per line. Future conical scanners will have many more samples per line, and the size of the input buffer will assume major importance.

The quality of the photographic products produced by this experiment were good (see Plate 1). They appeared to be about equal to LANDSAT photographs produced on the same equipment and in a similar manner.

This experiment has demonstrated that a conical scanner can be a viable choice for an earth observation sensor. Ground processing of conical data does require that large amounts of data be stored on fast access devices such as disks or computer memory. The choice of sensors, whether linear or conical, should be based primarily on sensor performance and cost.

UNANSWERED QUESTIONS

This experiment did not address several important topics pertaining to ground processing of conical scanner data:

- Terrain relief,
- Ground control point processing, and
- Large input data buffer,

Terrain relief is much more of a problem with a conical scanner than it is with a linear scanner due to the large scanning angle. It is probably necessary to correct for terrain relief in order to produce images that have precise geometric accuracy. It is also necessary to use ground truth information in order to obtain high geometric accuracy. Neither of these aspects has been considered in this investigation. The large buffer needed for conical data may be reduced in size by using a clever, efficient disk data management system. As yet, no such scheme has been tested.

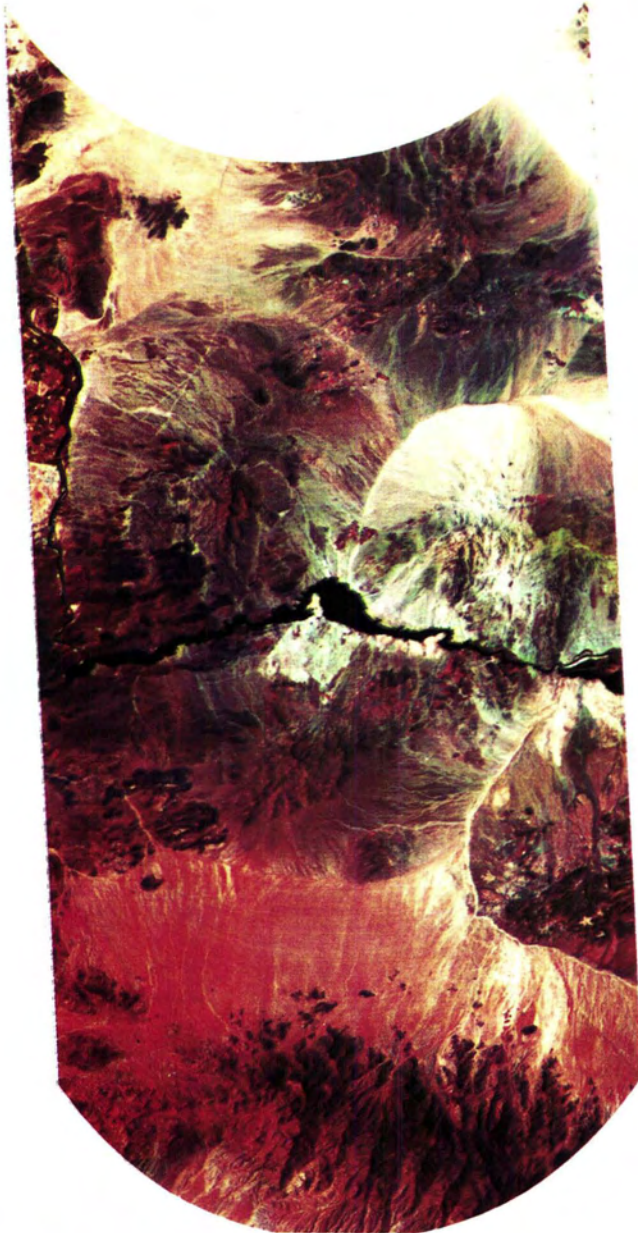
ACKNOWLEDGMENTS

The authors would like to thank several people from Honeywell Radiation Center in Lexington, Massachusetts for their assistance during the course of the S-192 experiment. They are D. A. Koso, M. F. Harris, H. W. Robinson, Jr., and O. E. Toler.

REFERENCES

- (1) NASA/Goddard Space Flight Center, *ERTS Data User's Handbook*, GE Document No. 71SD4249.
- (2) Bernstein, R. "Results of Precision Processing (Scene Correction) of ERTS-1 Images Using Digital Image Processing Techniques", *Symposium on Significant Results Obtained from the Earth Resources Technology Satellite-1*, Vol. II, NASA Document #SP-327, March 5-9, 1973.
- (3) Bernstein, R. "Scene Correction (Precision Processing) of ERTS Sensor Data Using Digital Image Processing Techniques", *Third ERTS Symposium*, Vol. 1, Section A, NASA SP-351, December 10-14, 1973.
- (4) Bernstein, R. *All-Digital Precision Processing of ERTS Images*, Final Report, NASA Contract NAS5-21716, April 1975.
- (5) NASA/Goddard Space Flight Center, *Master Data Processing (MDP) Systems*, RFP No. 5-70301-156, June 4, 1975.
- (6) NASA/JSC, *Earth Resources Production Processing Requirements for EREP Electronic Sensors*, PHO-TR524 Rev. B, June 1975.
- (7) NASA/Manned Spacecraft Center, *Earth Resources Data Format Control Book*, PHO-TR543, March 1973.

SKYLAB S192 IMAGE - LAKE HAVASU AREA
SYSTEM PROCESSED BY IBM ON 23 FEB 76

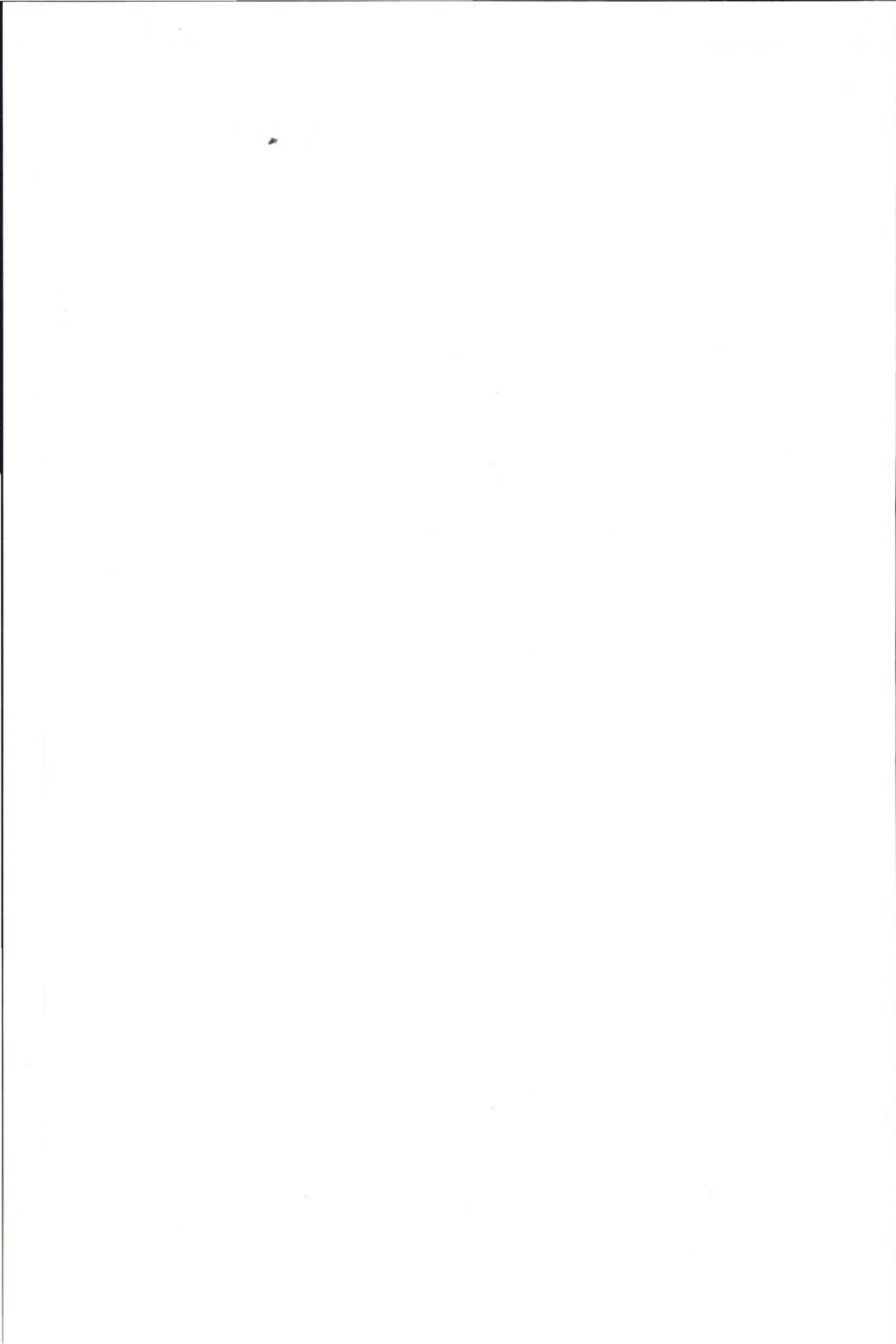


IMAGED AT 1805 GMT ON 15 SEP 73
LINE 73
MISSION 3
ORBIT 43
RUN 9

SPECTRAL BAND

VIOLET-BLUE
BLUE-GREEN
IR

Plate 1. Systematically processed S-192 image of Lake Havasu area.



- (8) Forrest, R. B., T. A. Eppes, and R. J. Ouellette, *EOS Mapping Accuracy Study*, Final Report for contract NAS-5-21727, March 1973.
- (9) Friar, M. E., R. D. Hogan, T. J. Min, J. V. Sharp, and D. R. Thompson, *System and Design Study for an Advanced Drum Plotter*, Final Technical Report, USAETL contract DAAK-02-69-C-0015, April 1970.

APPENDIX A
DEFINITIONS OF COORDINATE SYSTEMS (RIGHT-HANDED)

Notation	Terminology	Definition
X_s, Y_s, Z_s	Local sensor coordinates	Origin at spacecraft; X, Y, Z-axes determined by roll, pitch, and yaw relative to local earth-perpendicular axes.
X_p, Y_p, Z_p	Local earth-perpendicular coordinates	Origin at spacecraft; X-direction of spacecraft orbital vector; Z-axis normal to earth ellipsoid.
X_t, Y_t, Z_t	Local earth-tangent coordinates	Translate of local earth-perpendicular coordinates to spacecraft nadir point.
X_c, Y_c, Z_c	Local earth-centered coordinates	Origin at geocenter; X-axis in meridional plane of nadir; Z-axis is polar axis.

Membership Application

I hereby apply for Regular Membership in the American Society of Photogrammetry and enclose \$20.00* for _____ (year), or \$10.00* for period 1 July to 31 December, and \$_____ for a _____ Society emblem and/or membership certificate. (Send to ASP, 105 N. Virginia Ave., Falls Church, Va. 22046.)

First Name	Middle Initial	Last Name	Title
Mailing Address (Street and No., City, State, Zip Code and Nation)			County
Profession or Occupation		Present Employment	
<input type="checkbox"/> Reg. Prof. Engineer <input type="checkbox"/> Reg. Land Surveyor <input type="checkbox"/> Other Societies (List)		Position or Title	
(Please print or type on the lines above)			
Date	Signature of Applicant		
Date	Endorsing Member (Endorsement desired but not necessary)		

* Your dues payment covers your subscription to *Photogrammetric Engineering and Remote Sensing*.